

## Coupled electrostatic-elastic analysis for topology optimization using material interpolation

This article has been downloaded from IOPscience. Please scroll down to see the full text article.

2006 J. Phys.: Conf. Ser. 34 264

(<http://iopscience.iop.org/1742-6596/34/1/044>)

View [the table of contents for this issue](#), or go to the [journal homepage](#) for more

Download details:

IP Address: 38.107.179.214

The article was downloaded on 16/02/2012 at 02:40

Please note that [terms and conditions apply](#).

## Coupled electrostatic-elastic analysis for topology optimization using material interpolation

A Alwan and G K Ananthasuresh

Mechanical Engineering, Indian Institute of Science  
Bangalore 560 012, INDIA

aravindalwan@gmail.com, suresh@mecheng.iisc.ernet.in

**Abstract.** In this paper, we present a novel analytical formulation for the coupled partial differential equations governing electrostatically actuated constrained elastic structures of inhomogeneous material composition. We also present a computationally efficient numerical framework for solving the coupled equations over a reference domain with a fixed finite-element mesh. This serves two purposes: (i) a series of problems with varying geometries and piece-wise homogeneous and/or inhomogeneous material distribution can be solved with a single pre-processing step, (ii) topology optimization methods can be easily implemented by interpolating the material at each point in the reference domain from a void to a dielectric or a conductor. This is attained by considering the steady-state electrical current conduction equation with a ‘leaky capacitor’ model instead of the usual electrostatic equation. This formulation is amenable for both static and transient problems in the elastic domain coupled with the quasi-electrostatic electric field. The procedure is numerically implemented on the COMSOL Multiphysics® platform using the weak variational form of the governing equations. Examples have been presented to show the accuracy and versatility of the scheme. The accuracy of the scheme is validated for the special case of piece-wise homogeneous material in the limit of the leaky-capacitor model approaching the ideal case.

### 1. Background and Motivation

Electrostatic force is one of the most important means of providing actuation in microsystems owing its popularity primarily to its favorable scaling at the micron scale and adaptability to most micromachining techniques. Its widespread use has spawned a variety of analytical and numerical methods for its analysis (e.g., [1]) and shape optimization (e.g., [2]). The comparative speeds and accuracies of various analysis algorithms come under close scrutiny in design situations involving multiple, iterative analysis steps such as those encountered in topology optimization or in the manual design of complex microsystem devices.

To implement topology optimization for electrostatically actuated structures, a framework is required to allow any portion of a given region to be a conductor, dielectric, or void because every point can potentially be occupied by a conductor or a dielectric or by no material at all. Even though topology optimization-based synthesis methods have been reported for a variety of actuations in microsystems [3], such an attempt for electrostatically actuated microstructures is reported only recently [4]. The inability to smoothly interpolate the state of the material from a conductor to a dielectric or a void was perhaps a reason for this. In this paper, we introduce a new method for this purpose by modeling electrostatic domains as limiting cases of regions with spatially varying

conductivity. An additional advantage of the inhomogeneous conductivity model of the electrostatics problem is that it allows the flexibility to simulate arbitrary material composition within a given region of any shape and topology. Furthermore, the finite element mesh on the region can be fixed even when the internal geometries and interfaces change. This enables quick multiple runs with changed geometry, materials and other parameters, which expedites the re-design process without the trouble of repeated pre-processing.

## 2. New Analytical Formulation

In traditional coupled electrostatic-elastic analysis, a given domain is partitioned into regions composed of conductors with dielectrics and/or voids among them. By applying the electrical boundary conditions, we solve the Laplace equation in the void regions. The resulting electrostatic potential field ( $\Phi$ ) yields the distribution of surface charge density ( $\rho_s$ ) on the conductors' boundaries. This helps compute the electrostatic forces ( $\mathbf{f}_{es}$ ) on the interfaces, which are then used to solve for the elastic displacements ( $\mathbf{u}$ ) in the structural domain. The displacements so computed are coupled back into the electrostatic domain (because the domains  $\Omega_{void}$  and  $\Omega_{struc}$  would have changed now) and the cycle is repeated until a self-consistent solution is found. This process is illustrated in figure 1, where  $\varepsilon_0$  is the dielectric permittivity of free space,  $\mathbf{S}$  the elastic stress tensor and  $\mathbf{Y}$  the Young's modulus tensor of the material that forms the structure.

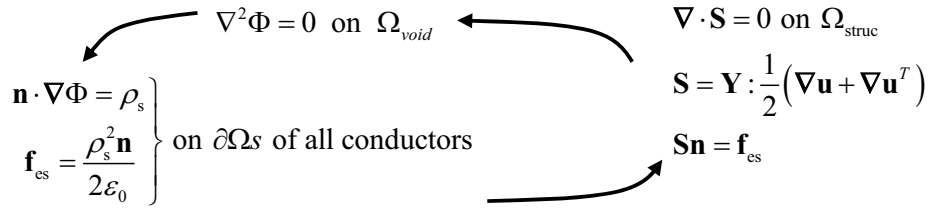


**Figure 1.** The traditional electrostatic-elastic analysis process

The framework shown in figure 1 serves well for shape optimization and size (or parameter) optimization in which the regions of conductors and voids are known a priori although the boundary may be changing. However, in topology optimization the internal geometries and interfaces among conductors, dielectric and voids are not known; in fact, they get determined during the process of optimization. As is well known in this field, topology optimization is equivalent to optimal material distribution [3, 5]. When continuous optimization algorithms are used, the material distribution needs to be varied smoothly. This calls for “material interpolation” where continuous “intermediate” state is defined in between the material and void states [6]. In this paper, we define the properties of such a smoothed material state in terms of a spatially-varying material selection parameter. In the limit, this leads to distinct selection of conductors and voids when suitable upper and lower bounds are imposed on this parameter. Conductor and void regions are thus demarcated by spatially varying values of this parameter in an iterative optimization procedure. The physical basis for such an interpolation model is explained next.

### 2.1. The leaky capacitor model

Consider a region of inhomogeneous conductivity with some arbitrary distribution of electric current flowing through it. Assuming the absence of sources and sinks of current, we consider the continuity equation for the volume density of free electric charge in the domain  $\rho_e$ , in terms of the electric current density vector  $\mathbf{J}$ .

$$\frac{d\rho_e}{dt} + \nabla \cdot \mathbf{J} = 0 \quad (1)$$

Substitution of the microscopic form of the Ohm's law (equation (2)) into equation (1), under steady-state conditions, gives the electric field distribution in a general conductive medium.

$$\mathbf{J} = \sigma \mathbf{E} \quad (2)$$

$$\nabla \cdot (\sigma \mathbf{E}) = 0 \quad (3)$$

Here,  $\sigma(x, y, z)$  is the spatially varying conductivity and  $\mathbf{E}$  is the electric field. In this model,  $\sigma(x, y, z)$  varies between zero (the case of void) and infinity (the case of an ideal conductor). Under the same set of electrostatic boundary conditions, a part of the region that is in between the two extremes would partially conduct current and store electrostatic energy. In lumped modeling, it is equivalent to a resistor and a capacitor in parallel. This is known as the *leaky capacitor model* [7]. In the limit, this model approaches a pure conductor in the desired parts and void regions elsewhere thus resulting in idealized capacitive configurations. In a more general case, dielectric materials can also be modeled by interpolating the permittivity in addition to the conductivity.

Similarly, in the mechanical problem, we represent the entire domain as a single material with spatially-varying elastic moduli (e.g., Young's modulus) to distinguish the voids from the conductor and dielectric regions. These moduli are incorporated into the elastostatic<sup>1</sup> governing equation

$$\nabla \cdot (\mathbf{S}) = \mathbf{F}_{es} \quad (4)$$

where  $\mathbf{S}$  is the stress tensor which is a product of constitutive elastic modulus tensor and the strain tensor. The *body force* term  $\mathbf{F}_{es}$  that appears in equation (4) is the electrostatic force per unit volume. The expression for this force is derived from the general electrostatic stress tensor [8] and may be stated as follows:

$$\mathbf{F}_{es} = \rho_e \mathbf{E} - \frac{1}{2} E^2 \nabla \varepsilon + \frac{1}{2} \nabla \left( E^2 \frac{\partial \varepsilon}{\partial \rho_m} \rho_m \right) \quad (5)$$

where  $\rho_e$  is the free electric charge density,  $\varepsilon$  is the permittivity and  $\rho_m$  is the mass-density of the material. The third term in equation (5) may be neglected in most practical situations since we are only concerned with the resultant forces on the domain [8]. Using the electrostatic Poisson equation (i.e.,  $\nabla \cdot (\varepsilon \mathbf{E}) = \rho_e$ ), the microscopic form of Ohm's law (equation (2)) and equation (3), we may alternatively rewrite the above force expression in the following form.

$$\begin{aligned} \mathbf{F}_{es} &= \nabla \cdot (\varepsilon \mathbf{E}) \mathbf{E} - \frac{1}{2} E^2 \nabla \varepsilon = \nabla \cdot \left( \frac{\varepsilon \mathbf{J}}{\sigma} \right) \mathbf{E} - \frac{1}{2} E^2 \nabla \varepsilon \\ &= \left( \frac{\nabla \varepsilon \cdot \mathbf{J}}{\sigma} - \frac{\varepsilon \nabla \sigma \cdot \mathbf{J}}{\sigma^2} + \frac{\varepsilon}{\sigma} \nabla \cdot \mathbf{J} \right) \mathbf{E} - \frac{1}{2} E^2 \nabla \varepsilon = \left( \nabla \varepsilon \cdot \mathbf{E} - \frac{\varepsilon \nabla \sigma \cdot \mathbf{E}}{\sigma} + 0 \right) \mathbf{E} - \frac{1}{2} E^2 \nabla \varepsilon \quad (6) \\ \Rightarrow \mathbf{F}_{es} &= \left\{ \left( \frac{\nabla \varepsilon}{\varepsilon} - \frac{\nabla \sigma}{\sigma} \right) \cdot (\varepsilon \mathbf{E}) \right\} \mathbf{E} - \frac{1}{2} E^2 \nabla \varepsilon \end{aligned}$$

Equation (6) clearly shows how the electrostatic force develops in regions where there is a variation in either conductivity or permittivity. In the limit of the entire domain being demarcated into conducting and void regions, we see that the electrostatic force automatically gets confined to the interfaces where there is a discontinuity in the material properties. Thus, the body force shown in equation (4) approaches the familiar electrostatic boundary force at the interfaces.

While the body force shown in equation (5) is readily implementable in a numerical scheme, an alternate procedure may be used when the entire domain is discretized into an array of cells. We would then assume that material properties remain constant inside each cell while being different from cell to cell. Then, the discontinuities arise only on the boundaries between adjacent cells. As a consequence, the electrostatic body force now transforms into an interface force that acts on the boundaries between cells [8]. The expression for this interface force per unit area is given as follows:

<sup>1</sup> For elastodynamics, on the left side we need to add the inertia term  $\rho_m \ddot{\mathbf{u}}$ , where  $\rho_m$  is the mass density of the material and  $\mathbf{u}$  is the displacement field.

$$\mathbf{F}'_{es} = D_{2n}\mathbf{E}_2 - D_{1n}\mathbf{E}_1 - \frac{1}{2}(D_2E_2 - D_1E_1)\mathbf{n} \quad (7)$$

where  $\mathbf{n}$  is the outward normal to the surface,  $\mathbf{D}$  the electric displacement field, and  $D_n$  its component normal to the surface, while the indices 1 and 2, respectively, refer to the quantities on the inner and outer sides of the surface. These procedures allow us to accurately compute the electrostatic force for any arbitrary material distribution.

### 2.2. Material interpolation

We define spatially-varying parameters  $\gamma_1$  and  $\gamma_2$  to smoothly interpolate conductivity, permittivity and elastic moduli ( $\mathbf{Y}$ ) of the entire domain. In general, there are four possible types of materials: a pure conductor with the dielectric constant close to unity ( $c$ ), a conductor with a dielectric constant significantly larger than unity ( $cd$ ), an insulating dielectric ( $d$ ) and air/void. In surface micromachined structures metals, polysilicon, silicon nitride/oxide and air gap respectively correspond to the above possibilities. Here,  $\gamma_1$  and  $\gamma_2$  should be interpreted as material selection parameters that interpolate and help choose a material at every point in the design domain. Referring to Table 1, the four types of materials can be interpolated as follows.

$$\begin{aligned} \sigma &= \sigma_0(1-\gamma_1) + \gamma_1\{\sigma_{cd}\gamma_2 + \sigma_c(1-\gamma_2)\} \\ \varepsilon &= \varepsilon_0(1-\gamma_2) + \gamma_2\{\varepsilon_{cd}\gamma_1 + \varepsilon_d(1-\gamma_1)\} \\ \mathbf{Y} &= \mathbf{Y}_0(1-\gamma_1)(1-\gamma_2) + \mathbf{Y}_d(1-\gamma_1)\gamma_2 + \mathbf{Y}_c\gamma_1(1-\gamma_2) + \mathbf{Y}_{cd}\gamma_1\gamma_2 \end{aligned} \quad (8)$$

It should be noted that  $\gamma_1$  and  $\gamma_2$  are bounded between zero and one. When they assume values at these bounds, we get four combinations as seen in the table. It is also important to note that the interpolating formulae in equation (8) reduce to this discrete selection with  $\gamma_1$  and  $\gamma_2$  at their bounds. When their values are in between, equation (8) helps define functionally graded materials. As mentioned earlier, this interpolation is also useful in topology optimization. After discussing the implementation of the new formulation in equations (3), (4) and (6) with material interpolation in equation (8), a few examples are presented to show that piecewise homogeneous material distribution can also be done in this manner. That is, it offers a convenient framework for solving the usual problems wherein the regions of conductors, dielectrics and voids are clearly demarcated.

**Table 1.** Materials and their properties relevant to the coupled electrostatic-elastic analysis

	Conductor: $c$	Conductor with permittivity: $cd$	Insulating dielectric: $d$	Air or void
$\gamma_1$	1	1	0	0
$\gamma_2$	0	1	1	0
$\sigma$	$\sigma_c$	$\sigma_{cd}$	$\sigma_0 \approx 0$	$\sigma_0 \approx 0$
$\varepsilon$	$\sim \varepsilon_0$	$\varepsilon_{cd}$	$\varepsilon_d$	$\varepsilon_0$
$\mathbf{Y}$	$\mathbf{Y}_c$	$\mathbf{Y}_{cd}$	$\mathbf{Y}_d$	$\mathbf{Y}_0 \approx \mathbf{0}$

### 3. Implementation

The numerical scheme is implemented in COMSOL Multiphysics® to solve the coupled electrostatic-elastic problem in a fixed rectangular domain with  $\gamma_1$  and  $\gamma_2$  represented by spatially varying functions. We note that these functions take values between zero and one over the entire domain so as to represent different types of materials as explained in the previous section. For a functionally graded or otherwise heterogeneous distribution of material, the functions will be defined appropriately. In topology optimization, an optimization algorithm determines these functions to minimize an objective

function subject some constraints. The third use of these functions is illustrated in this paper to conveniently model usual homogeneous conductor/dielectric/void regions with the sharp interfaces within the domain. For this, we define  $\gamma_1$  and  $\gamma_2$  through appropriate combinations of step functions, thereby outlining sharp interfaces between adjacent material types. Apart from creating well-defined material regions, sharp transitions also help in localizing the body force so that a meaningful comparison may be made with standard electrostatic analysis methods (as in figure 1).

However, the presence of spatial derivatives in electrostatic force density expression (see equation (6)) makes it necessary for the material properties to be differentiable with respect to the space dimensions. This is guaranteed by using smooth high-order sigmoid functions in place of discontinuous step functions in the expressions for  $\gamma_1$  and  $\gamma_2$ . We can thus ensure that the electrostatic force is resolved accurately by taking a finite element discretization that is small enough to interpolate these high-order sigmoid functions. Naturally, there exists a lower limit on the size of the finite element mesh due to limitations on the size of memory in a computer. This leads to a trade-off between the accuracy of force computation and the precision in defining material interfaces. However, it is not difficult to find appropriate extent of smoothness for the step functions through some numerical experiments. For the examples presented in the next section, we choose sigmoid functions of the form

$$\gamma = \gamma_{\min} + \frac{\gamma_{\max} - \gamma_{\min}}{1 + \exp\{-m(x - x_0)\}} \quad (9)$$

where  $\gamma_{\min}$  and  $\gamma_{\max}$  have values of zero and one respectively, while the value of  $m$  is chosen to be 40-80 times to that of  $x$ .

#### 4. Results

The accuracy of the material interpolation formulation was validated by solving a simple cantilever problem. The problem was solved using both the body force formulation of equation (6) (see figure 2) and the surface force formulation of equation (7) (see figure 3). The bottom edges of both the cantilever and the bottom plate were held fixed and a potential difference of 10 volts was applied across them. The deformation in the structure has been scaled up for ease of visualization. This solution compares well with the standard coupled electrostatic-elastic solver that was included in COMSOL Multiphysics® within an error of 0.1%.

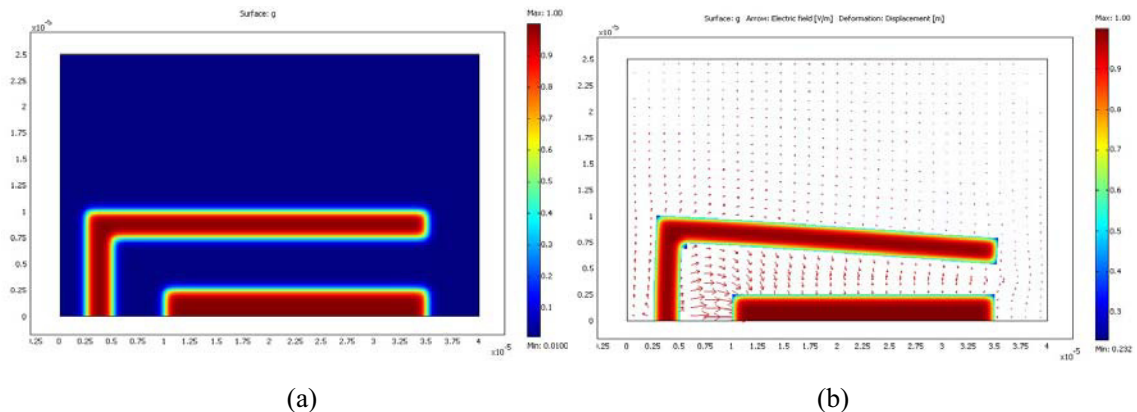


**Figure 2.** Deformation of a simple cantilever due to electrostatic force. (a) Plot of  $\gamma_1$  showing undeformed structure (b) Deformed structure with arrows indicating direction and magnitude of the electric field. Only mesh elements with  $\gamma_1$  greater than 0.5 have been shown for clarity .

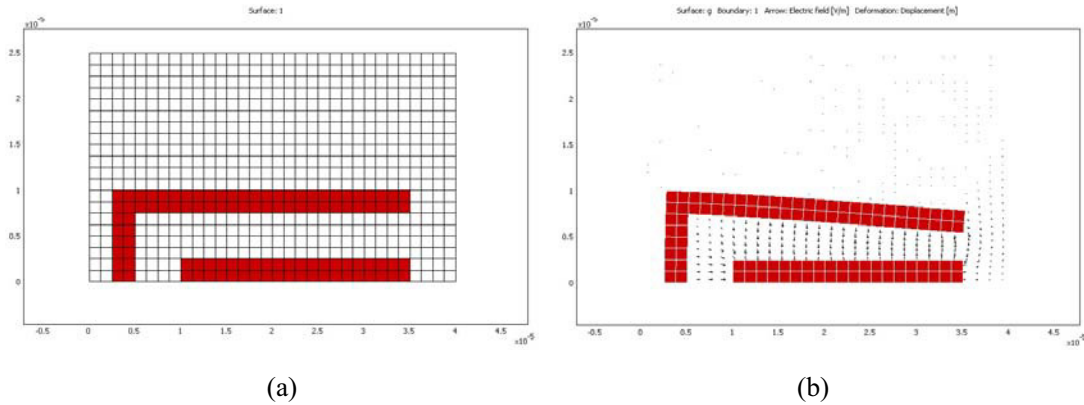


**Figure 3.** Deformation of a simple cantilever due to the electrostatic force – surface force formulation. (a) Undeformed structure (b) Deformed structure with arrows indicating direction and magnitude of electric field. Only mesh elements with  $\gamma_1$  greater than 0.5 have been shown for clarity.

The material interpolation formulation was also used to model a micromachined polychromator-like device [9], where a mirrored slender rectangular surface is to be translated vertically up and down using electrostatic force with minimal elastic deformation. We employed the innate symmetry in the problem to reduce the design domain by half, in order to improve computational accuracy. The symmetric right half of the undeformed structure is shown in figure 4(a). The feet of the moving structure are constrained and held at a potential difference of ten volts. The bottom electrode is constrained and electrically grounded. From figure 4(b), we see that only the vertical deflection of the mid-point of the fixed-fixed beam is transmitted to the flat mirrored surface at the top resulting in vertical motion without deformation.

Another well-known device that we modeled was a relay switch (figure 5), where an actuation electrode is used to deflect a cantilever, thereby making and breaking electrical contact between a pair of contact electrodes. The actuation electrodes are insulated from the contact electrodes by silicon nitride. This example shows how dielectric materials may be included in the analysis.

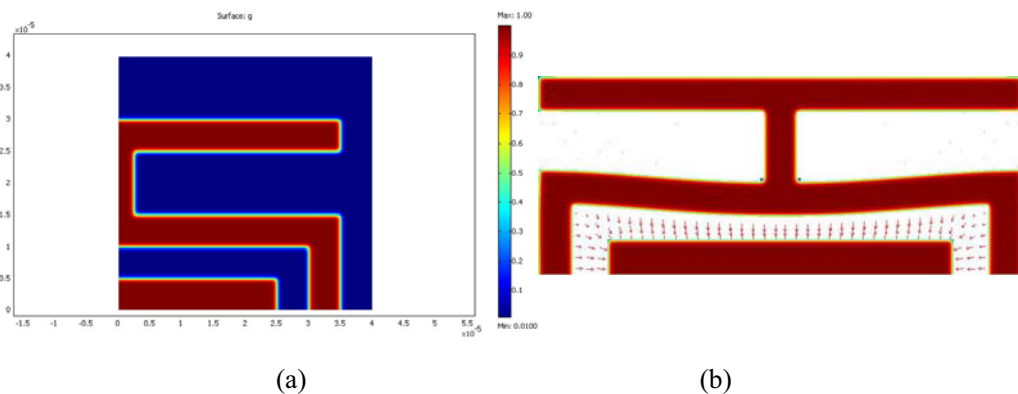


**Figure 4.** Analysis of a polychromator device in which electrostatic force is used to move a mirrored surface vertically without deformation (a) Plot of  $\gamma_1$  showing undeformed structure modeled using symmetry boundary conditions on the left edge (b) Complete deformed structure. Arrows indicate the direction and magnitude of electric field. Only mesh elements with  $\gamma_1$  greater than 0.5 have been shown for clarity.

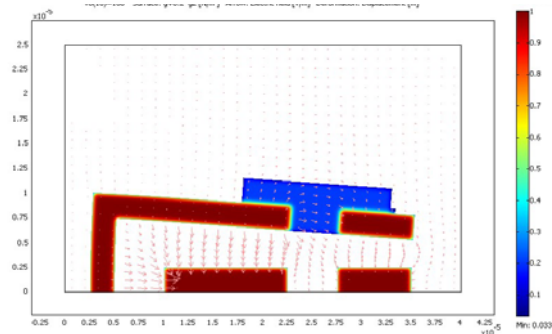


**Figure 5.** Analysis of a relay switch in which electrostatic force is used to make and break electrical contact. Red indicates polysilicon and light blue indicates silicon nitride that is used to electrically insulate the actuation mechanism and the switch contacts. Arrows indicate direction and magnitude of electric field. Only mesh elements with  $\gamma_1$  and  $\gamma_2$  greater than 0.5 have been shown for clarity.

## 5. Closure

The material interpolation model that we propose in this paper has a lot of flexibility in terms of performing electrostatic-elastic analysis for any arbitrary topology and material distribution, as is demonstrated in the three examples. Moreover, the leaky capacitor model that forms the physical basis for this formulation allows for accurate analysis not only in the limiting case of piecewise homogeneous material distributions, but also in all intermediate cases that represent functionally graded materials. This feature is also important in that it facilitates the implementation of optimal topology synthesis methods to optimize electrostatic actuator designs. The next step is to use this in topology optimization of surface-micromachined structures wherein polysilicon, nitride/oxide, and void regions can be smoothly varied to arrive at optimal topologies that obey the manufacturing constraints of a foundry process such as MUMPs [10]. This will be presented in our future publications.

## 6. References

- [1] Aluru N R and White J 1997 An efficient numerical technique for electromechanical simulation of complicated microelectromechanical structures *Sensors and Actuators A: Physical* **58**(1) pp 1–11.
- [2] Ye W and Mukherjee S 1998 Optimal shape design of an electrostatic comb-drive in MEMS *J. Microelectromech.* **7**(1) pp. 16-26.
- [3] Ananthasuresh G K (2003) *Optimal Synthesis Methods for MEMS* (Boston: Kluwer-Academic Publishers).
- [4] Raulli M and Maute K 2004 Topology Optimization of Electrostatic MEMS *Proc. 10th AIAA/ISSMO Conf. on Multidisciplinary Analysis and Optimization* (Albany, NY, 30 August – 1 September, 2004).
- [5] Bendsoe M P and Sigmund O 2003 *Topology Optimization Theory, Methods and Applications* (Berlin: Springer).
- [6] Bendsoe M P and Sigmund O 1999 Material interpolation schemes in topology optimization *Archives of Applied Mechanics* **69**(9-10) pp 635-654.
- [7] Haus H A and Melcher J R *Electromagnetic Fields and Energy* () pp 47-48.
- [8] Tamm I E 1976 *Fundamentals of the Theory of Electricity* (Moscow: Mir Publishers) pp 162-183.
- [9] Hung E and Senturia S D 1999 Extending the travel range of analog-tuned electrostatic actuators *J. Microelectromech.* **8**(4) pp. 407-505.
- [10] <http://www.memscap.com/memsrus/crmumps.html>